Shear wave anisotropy beneath the Aegean inferred from SKS splitting observations

C. P. Evangelidis,[1] W.-T. Liang,[2,3] N. S. Melis,[1] and K. I. Konstantinou[4]

Received 24 July 2010; revised 20 January 2011; accepted 31 January 2011; published 28 April 2011.

[1] SKS splitting parameters are measured in the Aegean region using events recorded at a dense temporary network in the south Aegean and the operating permanent networks, especially focusing in the back-arc and the near-trench areas of the Hellenic arc. In general, fast anisotropy directions are trench perpendicular in the back-arc area and trench parallel near the trench. Anisotropy measurements near the volcanic arc mark the transition between these two regions. In the back arc, a gradual increase is observed in delay times from south to north, with a prevailing NE-SW direction. In Cyclades, this pattern is correlated with GPS velocities and stretching lineations of metamorphic core complexes. Our preferred source of anisotropy in the back-arc region is the mantle wedge flow, induced by the retreating descending slab. The westernmost termination of the trench reveals directions parallel with the Kefalonia Transform Fault and perpendicular to the convergence boundary. Beneath Peloponnese, the trench-parallel flow is probably located beneath the shallow-dipping slab, although scattered measurements may also reflect fossil anisotropy from a past NW-SE strike of the trench. In western Crete, which may be entering a stage of continental collision, the anisotropy pattern changes to trench perpendicular, with a possible subslab source. Good nulls in central east Crete indicate a change in the anisotropy origin toward the east. At the easternmost side of the trench, fast directions are trench parallel. This reflects a similar subslab flow that may become toroidal around the slab edge beneath western Turkey. This may also produce a trench-parallel flow within the mantle wedge.

Citation: Evangelidis, C. P., W.-T. Liang, N. S. Melis, and K. I. Konstantinou (2011), Shear wave anisotropy beneath the Aegean inferred from SKS splitting observations, *J. Geophys. Res.*, *116*, B04314, doi:10.1029/2010JB007884.

1. Introduction

[2] The Aegean region is characterized as a complex tectonic area resulting from the interaction between Africa and Eurasia convergence, the SW motion of Anatolia, and the large extension affecting the Aegean due to the slab retreat (Figure 1). As the African plate moves northward at a rate of 1 cm yr^{-1}, it subducts along the Hellenic trench and forms an active volcanic arc and a Wadati-Benioff zone extending down to a depth of 180 km [e.g., *Papazachos et al.*, 2000]. Complementary, Anatolia is extruded westward and its relative motion with Eurasia to the north is accommodated along the strike-slip system of the North Anatolian Fault (NAF). The slab retreat of the subducted African plate the last 30–35 Ma [e.g., *Wortel and Spakman*, 2000] causes a southward motion of the Hellenic active margin and a substantial extension of the overriding lithosphere (Figure 1). *McClusky et al.* [2000], using geodetic measurements, found that the southwestern Aegean-Peloponnese moves toward the S-SW relative to Eurasia, at 3 cm yr^{-1} in a coherent fashion, with low internal deformation. The largest part of the back-arc Aegean area is dominated by normal faults with an E-W trend and N-S extension, like the well defined Corinth rift (Figure 1). The westernmost termination of the Hellenic trench is the Kefalonia Transform Fault (KTF) [*Louvari et al.*, 1999], where the plate boundary is offset eastward. Further north, the collision between northwestern Greece and the Apulian platform in the west takes place [e.g., *Taymaz et al.*, 1991]. The easternmost end of the trench is a rapidly deforming zone with a spreading component along the arc of around 1 cm yr^{-1} [*Le Pichon and Kreemer*, 2010]. The area shows complex kinematics, probably different at shallow depth and in the mantle, with a prominent stress heterogeneity expressed at all depths [*Rontogianni et al.*, 2011]. In the south, the Mediterranean Ridge, a pronounced topographic high of deformed sediments, is the accretionary complex of the ongoing developing continental collision between Eurasia, Africa and the southwestward fast moving Aegean [*Kreemer and Chamot-Rooke*, 2004, and references therein]. Between Crete and the Mediterra-

[1]Institute of Geodynamics, National Observatory of Athens, Athens, Greece.
[2]Institute of Earth Sciences, Academia Sinica, Taipei, Taiwan.
[3]Institute of Oceanography, National Taiwan University, Taipei, Taiwan.
[4]Institute of Geophysics, National Central University, Jhongli, Taiwan.

0148-0227/11/2010JB007884

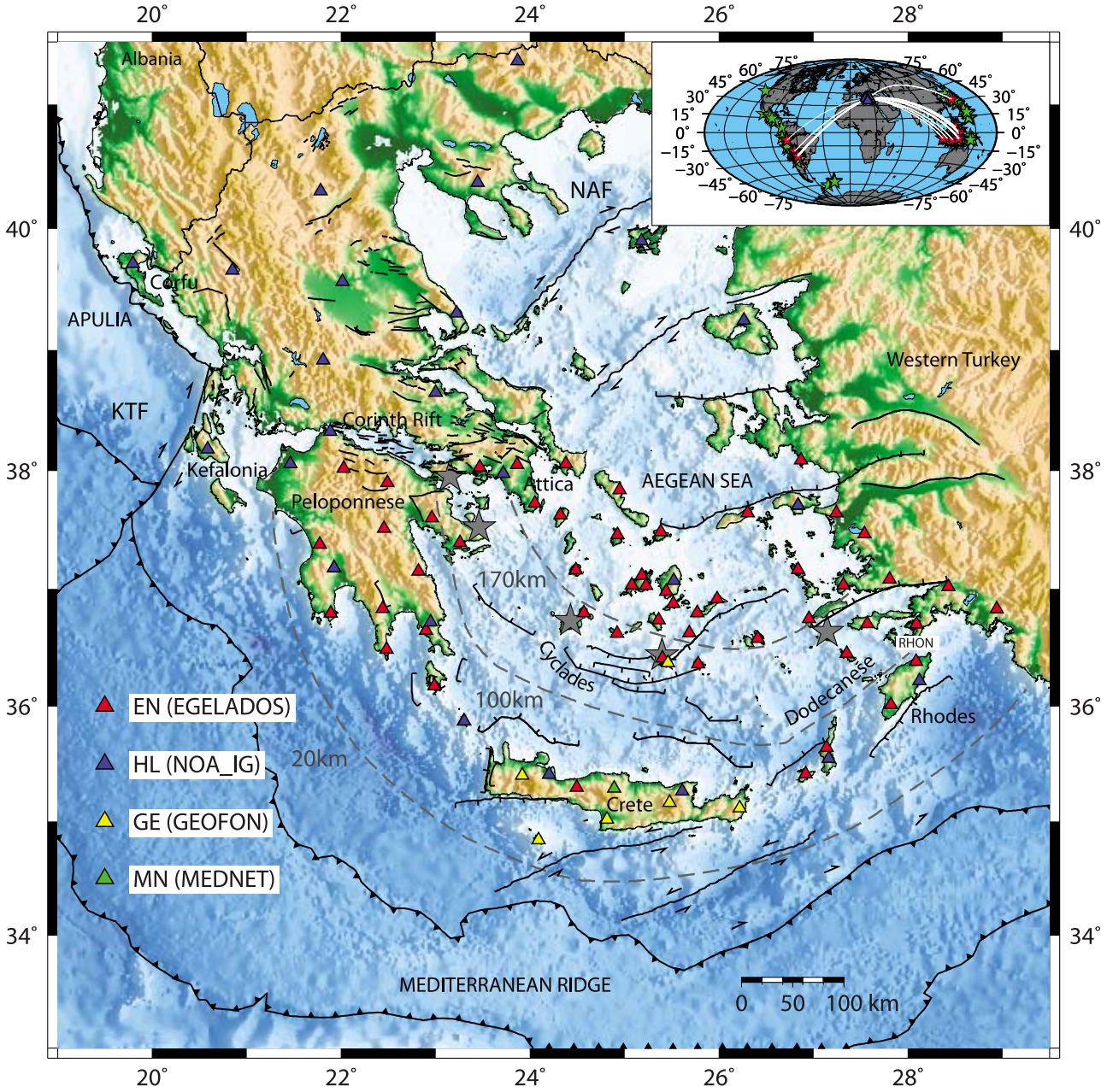

Figure 1. Main tectonic features of the broader Aegean Sea and the Hellenic trench region. Plotted faults are from *Chamot-Rooke et al.* [2005] and A. Ganas (personal communication, 2010). Gray dashed lines indicate isodepth curves for earthquake foci at 20 km, 100 km, and 170 km after *Papazachos et al.* [2000]. Gray stars indicate the active volcanic arc. Triangles mark broadband seismic stations used in this study in different colors according to the corresponding network. Name of station RHON, referred to in Figure 2, is given. KTF, Kefalonia Transform Fault; NAF, North Anatolia Fault. Inset map shows the spatial distribution of the teleseismic events analyzed. From those, events that provide acceptable SKS splitting parameters are marked in red.

nean Ridge, several segmented bathymetric troughs are the expression of left-lateral strike-slip motion within the fore arc [*Huguen et al.*, 2001].

[3] Apart from the intermediate depth earthquake studies that map the subducted slab, seismic tomography studies show also a high-velocity body turning around the Hellenic arc. This body is the subducted oceanic slab that can be followed down to at least the upper/lower mantle transition zone [e.g., *Wortel and Spakman*, 2000; *Piromallo and Morelli*, 2002]. *Konstantinou and Melis* [2008] based on shear wave propagation study suggested that the slab is continuous downdip for the depth range between 60 km and 160 km. Various tomography studies indicated a slab detachment below Peloponnese and a slab tear somewhere between Peloponnese and Crete [e.g., *Spakman et al.*, 1988; *Meijer and Wortel*, 1996]. Further east the slab is imaged

continuously. Between Rhodes and Cyprus the slab is again detached from its upper portion and its rupture may be prolonged until the Hellenic trench [*Faccenna et al.*, 2006]. *Brun and Sokoutis* [2010] suggested the slab is torn apart somewhere below southwestern Turkey, perpendicular to the direction of convergence.

[4] The most likely mechanism that generates seismic anisotropy in the mantle is lattice preferred orientation (LPO) of the anisotropic olivine crystals. When an aggregate of olivine is deformed in simple shear in the dislocation creep regime, it will develop an LPO (A-type olivine fabric) where the maximum concentration of fast axes will align with the direction of maximum shear [*Maupin and Park*, 2007]. On the other hand, when olivine is deformed at relatively high stresses and low temperatures in the presence of water, B-type fabric dominates and in this case the fast axes of olivine tend to align 90° away from the maximum shear direction in the shear plane [*Jung and Karato*, 2001].

[5] In subduction systems, possible sources that contribute to shear wave splitting are the overriding plate, the mantle wedge, the slab, and the subslab mantle. Beneath the wedge, fast directions are generally trench parallel, due to trench-parallel subslab mantle flow induced by trench migration [e.g., *Long and Silver*, 2008]. However, there are convergent boundaries, like the Cascadia subduction zone, where trench-perpendicular anisotropy was attributed to a similar subslab flow [*Currie et al.*, 2004]. In the mantle wedge, fast directions are usually complex, but often show a characteristic change in orientation from trench perpendicular in the back-arc region, due to the corner flow induced by the subducting slab, to trench parallel close to the trench. This change in orientation close to the trench has been mainly interpreted as being due to the presence of B-type olivine or serpentinite fabric in the cold corner of the mantle wedge [e.g., *Karato and Wu*, 1993; *Nakajima and Hasegawa*, 2004], the trench-parallel mantle wedge flow [*Smith et al.*, 2001], and complex 3D flow due to lower crustal foundering [*Behn et al.*, 2007].

[6] SKS wave splitting is the most useful tool to investigate upper mantle anisotropy, as these phases travel near vertically through the anisotropic material and the fast direction reflects the azimuth of the fast wave propagation in the horizontal plane [e.g., *Savage*, 1999; *Long and Becker*, 2010]. Previous SKS anisotropy studies in the Aegean include *Hatzfeld et al.* [2001], who used data of several temporary networks, concentrated mainly in central and northern Aegean. They concluded that the anisotropy is not associated with the tectonic fabric or the present-day Aegean motion, but it is correlated with the present-day strain field. They also suggested that the results could be obscured by the subduction regime.

[7] *Schmid et al.* [2004] also analyzed data from temporary and permanent stations mainly on Crete and the south Aegean region. They concluded that splitting is relatively small with a possible shallow origin. On Crete, laterally incoherent fast axes were attributed to the proximity of the slab and the strong structural heterogeneity. Measurements at central Aegean were parallel with the direction of back-arc extension and with the approximate movement of the Aegean microplate. Finally, *Kreemer et al.* [2004], based on the measurements of *Hatzfeld et al.* [2001], found an anticorrelation between crustal thickness and published anisotropy delay times, and a correlation with finite strain orientation, mainly accumulated in the Miocene.

[8] All previous studies do not incorporate significant number of measurements in the south Aegean region near the Hellenic trench boundary. In this study, we analyze SKS phases recorded at a dense temporary network in south Aegean and the backbone seismic networks that permanently operate in Greece. We especially focus on the back-arc and the near-trench areas where the density of our measurements is the largest. We interpret this shear wave splitting data set, integrating all available information for the Aegean region, which includes GPS velocities, the current strain field, metamorphic core complexes stretching lineations, along with 3D velocity structure from tomography studies and lithospheric boundaries derived from receiver functions.

2. Waveform Data and Splitting Analysis

[9] We analyze SKS phases from teleseismic events observed at epicentral distances between 80° and 120° and recorded at temporary deployed and permanent seismic broadband networks. The temporary deployed EGELADOS seismic network covered the south Aegean region from Peloponnese to western Turkey [*Friederich and Meier*, 2008]. Successive deployments resulted in a total of 54 stations, recording during the time period from November 2005 until March 2007 (Figure 1). For this period, 14 out of 34 teleseismic events examined have been qualified for SKS splitting analysis, after careful visual inspection. We also analyze SKS phases recorded from the permanent backbone seismic networks that span the entire Aegean-Greece region (Figure 1). For the same events we use 25 stations from the National Observatory of Athens Hellenic Broadband Seismic Network (HL), 6 stations from the GEOFON Network (GE) and 1 from the MedNet Network (MN). This study is complemented by the addition of 66 (out of 68) deep events from 2003 to 2008 for similar epicentral distances, that have been recorded by the permanent stations only.

[10] We measure the splitting parameters (ϕ, δt) of the SKS phase by applying particle motion analysis and using the cross-correlation method [*Fukao*, 1984], assuming that the splitting is generated from a single anisotropic layer. The two horizontal components are rotated in the horizontal plane at 1° increment from −90° to 90° and cross correlated in the selected SKS time window, with 0.01 s time shift increment. When the absolute cross-correlation coefficient is maximum, the rotation direction (ϕ) is the fast polarization direction and the time lag (δt) is the delay time of the slow shear wave (Figure 2). We accept results only when the S/N ratio is higher than 3 and the absolute cross-correlation coefficient is higher than 0.9. Finally, we calculate the 95% confidence interval of each solution using the interval estimate for the cross-correlation coefficient [*Rau et al.*, 2000]. We assign the errors for both ϕ and δt as the extreme values of the border of this confidence region (Figure 2 and Table S1 in the auxiliary material).[1] The mean ϕ error is 15°, whereas the mean δt error is 0.18 s. To assess the reliability

[1] Auxiliary materials are available in the HTML. doi:10.1029/2010JB007884.

RHON 2006 11 13 1:20

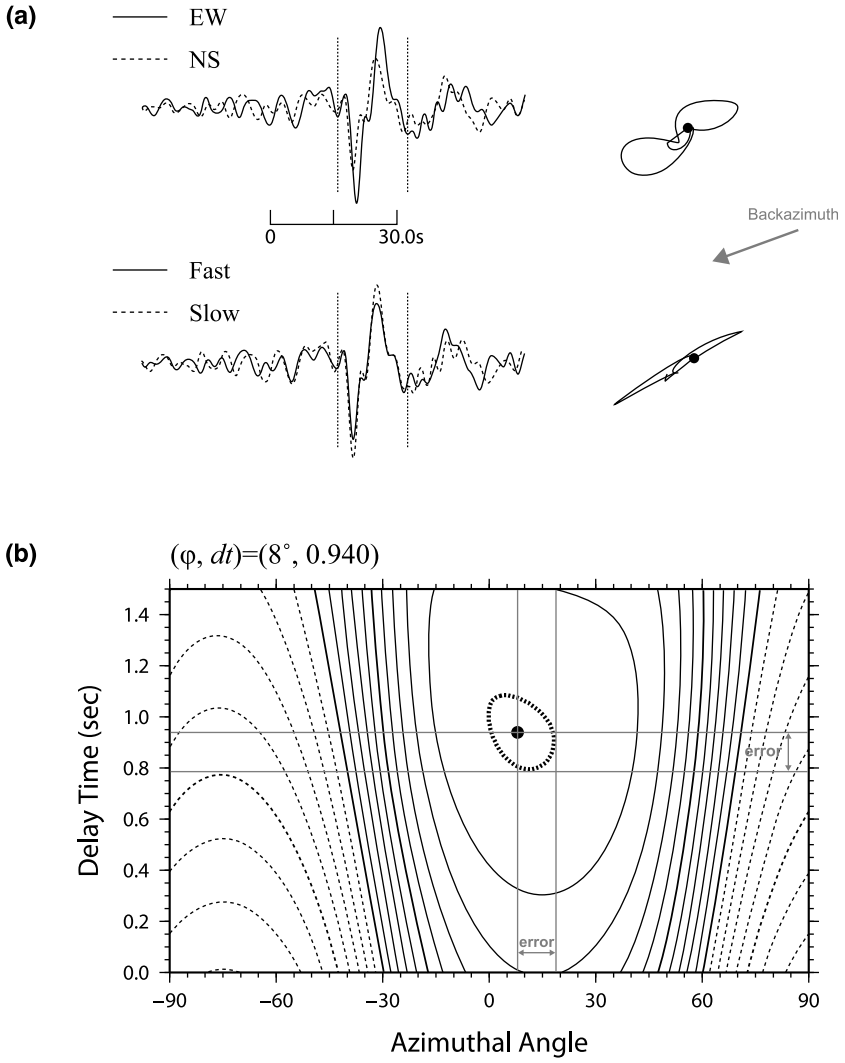

Figure 2. An example of measurement from an SKS phase recorded at station RHON for the event at 13 November 2006 01:20. (a) The upper two traces are the superposition of E-W (solid line) and N-S (dashed line) components. The lower two are the corrected fast (solid line) and slow (dashed line) components. Vertical dashed lines on the seismograms mark the intervals used to make the measurement. Corresponding particle motions and the back azimuth between the station and the event hypocenter are shown on the right. (b) A diagram of the distribution of the cross-correlation coefficients in (ϕ, δt) space. The estimated solution corresponding to the maximum value (dot) is shown with the 95% confidence region (thick dashed line); dashed contours indicate negative coefficient. Gray lines show the assigned errors of both ϕ and δt as the extreme values of the border of this confidence region.

of the method employed to calculate the anisotropy components, we identified two sets of earthquakes with near identical locations (event doublets) at different origin times. Differences in the estimated ϕ and δt at the same stations are less than 2° and 0.1 s, respectively (Figure 3 and Table S1).

3. SKS Splitting Azimuths and Delays

[11] In total, we estimate 133 non-null splitting parameter pairs (ϕ, δt), following the assigned selection criteria (Table S1). Out of the 80 analyzed events only 17 gave us acceptable results (Table S2 and Figure 1). We define as null measurements all those pairs that have δt lower than 0.2 s and those that have a S/N ratio higher than 5. Out of 32 null measurements only 20 do not show energy on the transverse component of the original seismograms. These pairs are accepted as good null measurements (Table S1). We also calculate the average ϕ and δt at each station by weighting each measurement with the reciprocal of its corresponding error (Table S3 and Figure 4).

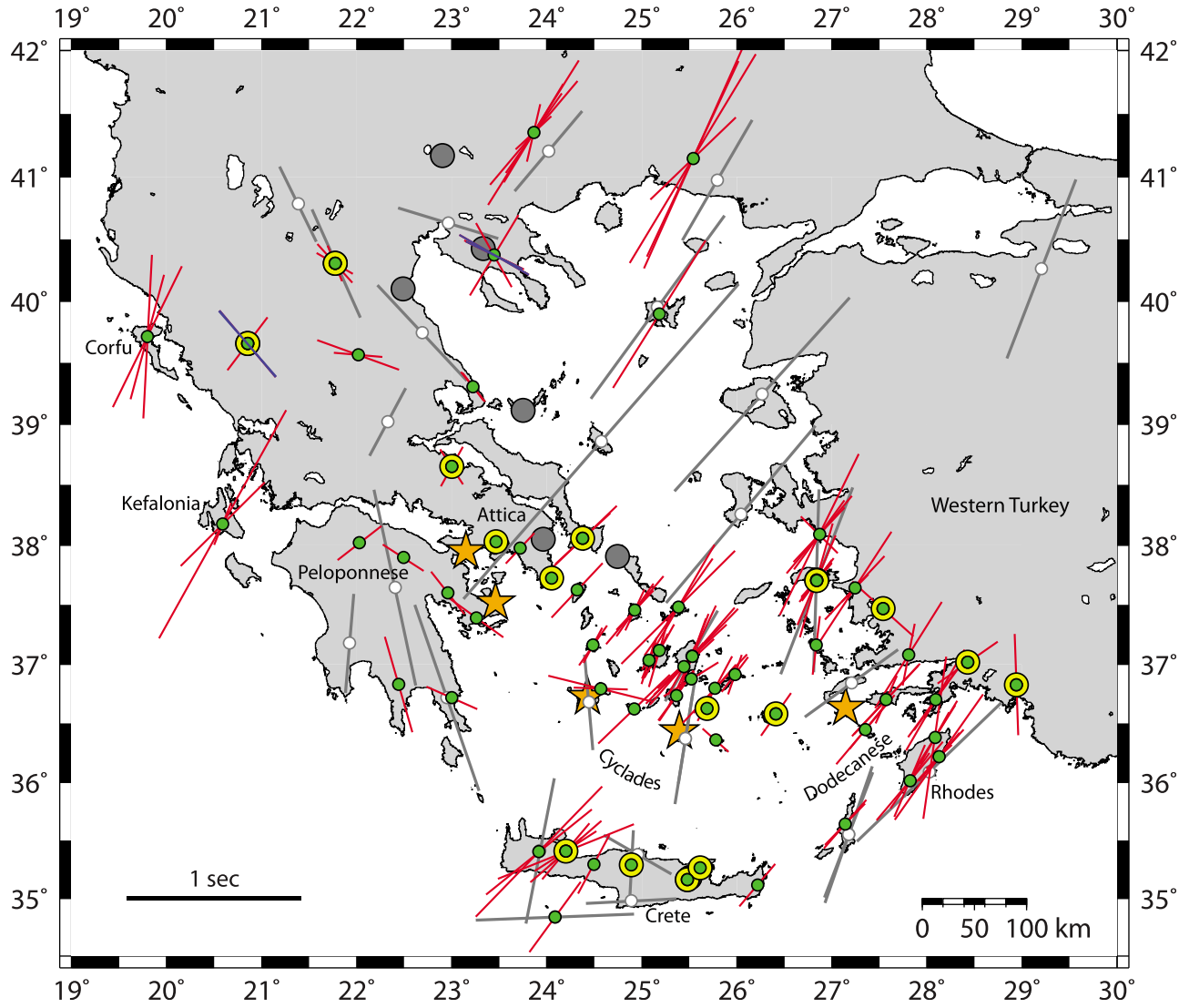

Figure 3. Map of SKS splitting results (ϕ, δt) displayed at each station. Red color bars indicate results from the present study and gray from previous studies, respectively. Large yellow and gray circles indicate good null measurements by this and previous studies, respectively. Permanent and temporary stations of this study with good splitting measurements are marked in green. Blue thin bars at two stations in the north show event doublets. Orange stars indicate the active volcanic arc.

[12] In general, there is a NE-SW trend in the Cyclades and the neighboring coast of Turkey with delay times between 0.2 and 1 s (Figures 3 and 5). The northern Aegean and the northeastern parts of Greece follow a similar pattern of fast directions with larger δt than 1 s (Figure 3). In Crete, there is a clear difference between the western side, with NE-SW trend as in the Cyclades (Figure 3), and the central eastern side with nulls. These good null measurements are in agreement with previous studies [see *Hatzfeld et al.*, 2001]. The fast directions in the Dodecanese islands and the southwestern Turkey, at the eastern side of the Hellenic trench, follow a trend similar to the Cyclades NE-SW direction, but also being parallel to the trench (Figures 3, 4, and 5). The fast directions at the Ionian islands reveal a NNE-SSW trend (Figure 5). At Kefalonia Island they are parallel to the KTF strike-slip fault (Figure 4). Similar trends with delay time higher than 0.8 s are also observed at the northwestern parts of the Hellenic peninsula, at Corfu Island. A small number of acceptable splitting measurements exist in the remaining areas of the Hellenic peninsula (Figure 3). In Peloponnese and the western parts of mainland Greece, the pattern is scattered but follows on average a NNW-SSE direction (Figure 5).

[13] Apart from central Crete, good nulls are located close to the volcanic arc, in the southwestern coast of Turkey and around Attica (Figure 3). Two good nulls in the mainland have initial polarization direction parallel to their overall fast or slow direction deduced from other measurements. Moreover, all good nulls measurements show similar directions to the non-null measurements (Figure 5), implying a simple anisotropic layer [e.g., *Buontempo et al.*, 2008].

[14] A visual comparison with the results of *Hatzfeld et al.* [2001] reveals some differences in both ϕ and δt (Figure 6). However, it should be noted that we use the

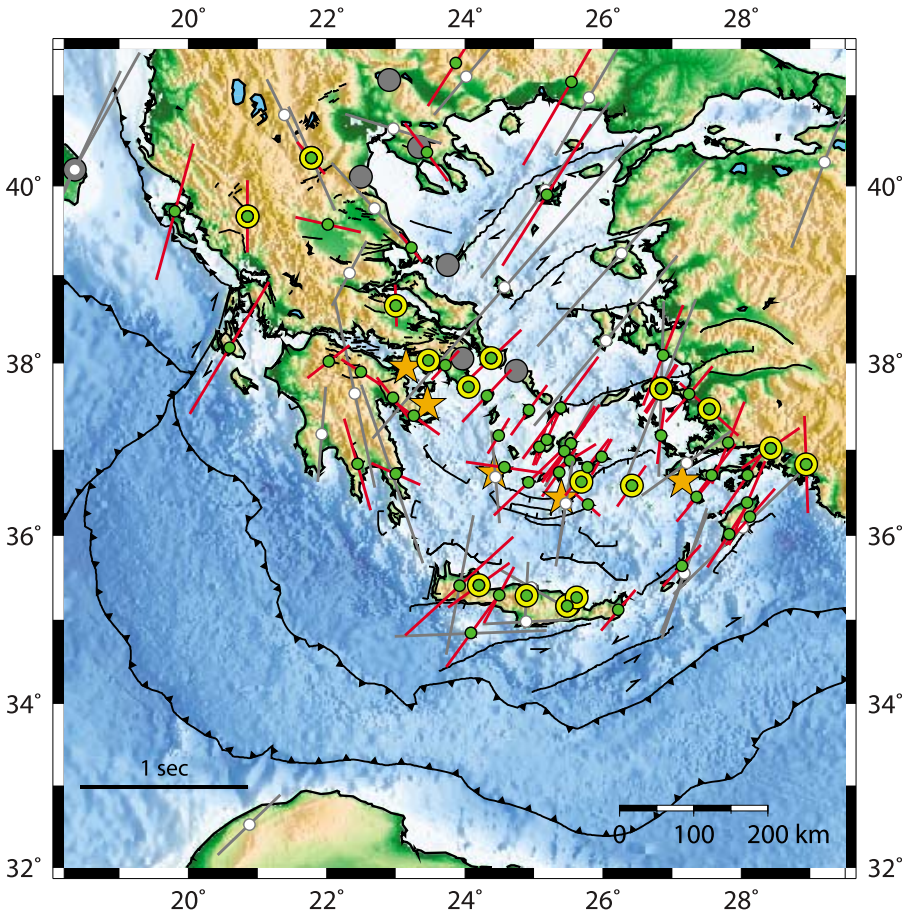

Figure 4. Map of weighted average SKS splitting results (ϕ, δt) displayed at each station (this study, red bars; previous study, gray bars) superimposed on a greater tectonic map of the area. Previous SKS splitting studies include those of *Hatzfeld et al.* [2001], *Schmid et al.* [2004], and *Baccheschi et al.* [2007]. Large yellow and gray circles indicate good null measurements by this and previous studies, respectively. Permanent and temporary stations of this study with good splitting measurements are marked in green. Main faults are similar with Figure 1. Orange stars indicate the active volcanic arc.

cross-correlation method (CCM) [*Fukao*, 1984], while *Hatzfeld et al.* [2001] use the method of rotating and minimizing one of the components of motion (MINM) and effectively removing the effect of anisotropy [e.g., *Vinnik et al.*, 1989]. The outcome of the anisotropy analysis is method dependent especially in areas that raypaths cross the mantle wedge [*Levin et al.*, 2007]. Close to the wedge tip the CCM method gives small δt but directions similar to those expected, whereas the MINM method gives large δt and fast direction at high angles to the expected orientation. In the case of corner flow in the mantle wedge, the differences between the two methods become larger.

[15] Another difference between this study and the one of *Hatzfeld et al.* [2001] is the error discrepancies (Figure 6). The greater quantity of measurements and the denser network coverage in the central Aegean, allow us to follow a more strict procedure in the choice of acceptable measurements. This is the reason for smaller errors in both ϕ and δt, although the way we calculate them differs from this of *Hatzfeld et al.* [2001]. *Monteiller and Chevrot* [2010] found that the errors in the MINM method are quite significant, even on high-quality records, because the measurement procedure involves the comparison of radial and transverse components, which are both contaminated by noise. To decrease the level of noise in the data, they recommend to average splitting intensities from waves coming from the same back azimuth. Taking all of the above into consideration we conclude that the fast directions of this study are within the error limits of *Hatzfeld et al.* [2001]. Delay times may differ due to the different methodologies in estimating anisotropy parameters, but the overall trend remains similar.

4. Aegean Mantle Anisotropy

[16] In general, most of the anisotropy measurements, based on their delay times, reveal an upper mantle origin [*Savage*, 1999]. However, a uniform pattern across the complex highly curved Hellenic subduction zone should not be expected. As *Savage* [1999] suggested, the three-dimensional nature of anisotropy should be considered in this kind of comparisons. Here, we focus on the possible source and directional pattern of the observed anisotropy, concentrated mainly in the back-arc domain in the central Aegean and the near-trench domain from western Greece,

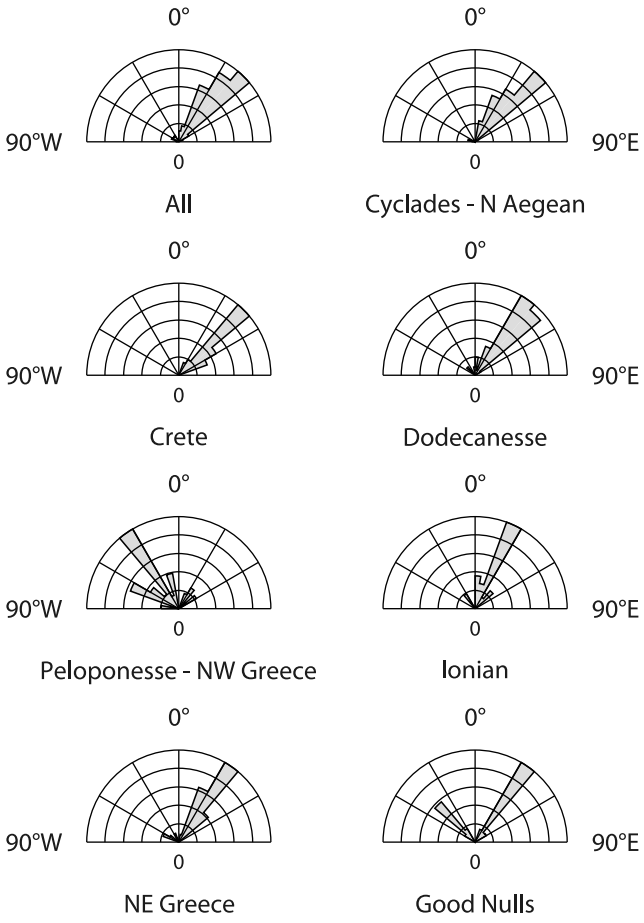

Figure 5. Polar histogram plots for all anisotropy measurements and for the six independent regions separately. The trend of each section represents the azimuth ϕ of the fast split shear wave, and the length is proportional to the number of measurements of ϕ at the same 10° intervals. A polar histogram of the assigned good nulls (that have δt values between 0 and 0.2 s) is also plotted.

to Peloponnese, Crete and the southeastern Aegean near Dodecanese.

4.1. Back-Arc-Induced Anisotropy

[17] Although *Hatzfeld et al.* [2001] suggested a consistency between the instantaneous strain field deduced from GPS measurements and the SKS fast splitting directions, there are systematic discrepancies between the two sets of directions (Figure 7a). Active extension trends more toward N-S direction than the SKS fast directions. *Kreemer et al.* [2004], based on the stretching orientation on metamorphic core complexes (MCC), suggested that the anisotropy in the lithospheric mantle is the result of the long period of extension during the Miocene and that the present-day crustal strain rate field is not associated with it. Comparing anisotropy directions with present strike of MCC stretching lineations show again discrepancies (Figure 7a). However, when their position is restored for paleomagnetic rotations [*Morris and Anderson*, 1996], they seem to have a good correlation with the corresponding anisotropy directions. Unfortunately, this information is available only for two islands in Cyclades (Figure 7a). On the other hand, GPS displacement vectors relative to a stable Eurasia taken from *Nyst and Thatcher* [2004], *Reilinger et al.* [2006], *Hollenstein et al.* [2008], and *Floyd et al.* [2010] are subparallel with the fast polarization directions of anisotropy only for the central and southeastern Aegean (Figure 7b). There are significant discrepancies between GPS velocity vectors and anisotropy directions in the back-arc regions of Peloponnese, southwestern Turkey and northern Aegean.

[18] *Jolivet et al.* [2009], based on the observation that the MCC stretching lineations are parallel with the anisotropy in the back-arc region, suggested that the crustal deformation in back-arc Aegean is mainly driven by the mantle flow from below. *Brun and Sokoutis* [2010] have also suggested that, in north and central Aegean, crust and mantle have experienced the same direction of flow the last 45 my, as the slab retreated through clockwise rotation around a vertical axis located in Albania (Figure 1). Whether the mantle flow and the crustal motion deformation couple or not it is not clear from this study.

[19] The thickness of an assumed single layer with 5% anisotropy, is estimated to be about 45 km and 90 km for 0.5 s and 1 s delay times, respectively [*Wolfe and Solomon*, 1998]. For the Cyclades, receiver functions estimates reveal a wedge 80 km thick at the volcanic arc, that thickens up to 140 km at northern Cyclades (Figure 8). At northern Aegean, tomography images show the cold slab that dips steeply and forms the main volume of the Aegean mantle wedge (Figure 9, cross section BB′). Therefore, the small anisotropy delay times in Cyclades may be produced by this thin wedge. The trench-perpendicular anisotropy pattern in the back-arc area is observed in many subduction zones and is mainly attributed to 2D corner flow induced by the downdip motion of the retreating slab. As the thickness of the anisotropic mantle wedge increases toward the north, the observed delay times in this study and those of *Hatzfeld et al.* [2001] also increase to higher values in the northern Aegean (Figures 8 and 9).

[20] Close to the volcanic arc and directly southward this NE-SW anisotropy changes to a pattern subparallel to the arc, that shows small delay times and null measurements. Due to the normal absence of islands south of the volcanic arc, this is mainly evident in few measurements in northeastern Peloponnese and south of the easternmost part of the volcanic arc, close to Turkey (Figure 4). We suggest that the Hellenic volcanic arc marks the transition between the back-arc-induced anisotropy to the trench-induced anisotropy, as it is globally observed [*Long and Silver*, 2008, and references therein].

4.2. Trench-Induced Anisotropy

[21] In general, the Hellenic arc is an arc of high curvature, strong 3D structure heterogeneities and different ongoing geodynamic processes. Therefore, a consistent and simple anisotropy pattern that would explain all observations near the trench is difficult. In the following, we try to analyze, for each different region near the trench, all possible explanations that could fit the data, starting from the two edges of the Hellenic arc and ending up to the central parts, in Peloponnese and Crete.

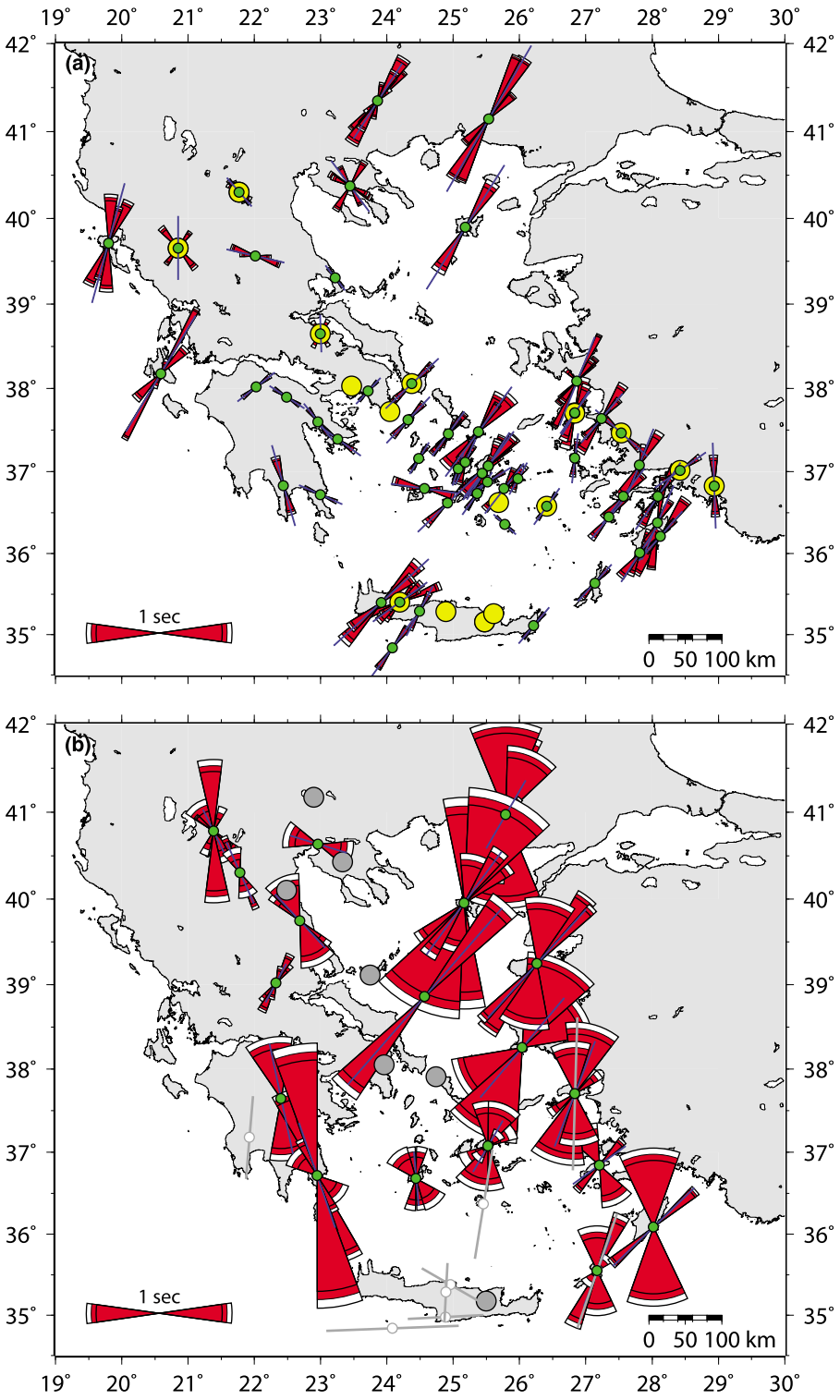

Figure 6. Maps showing splitting parameters that were derived (a) by this study and (b) by *Hatzfeld et al.* [2001]. Wedge width is proportional to the assigned error of the fast axis direction, whereas white areas outside of the wedges are proportional to half of the assigned error of the splitting time. Blue thin bars show the weighted mean at each station for both studies. Gray thin bars in Figure 6b show the mean SKS measurements at each station from the study of *Schmid et al.* [2004] where no individual measurements could be retrieved. Yellow and gray circles indicate good null measurements by this and previous studies, respectively.

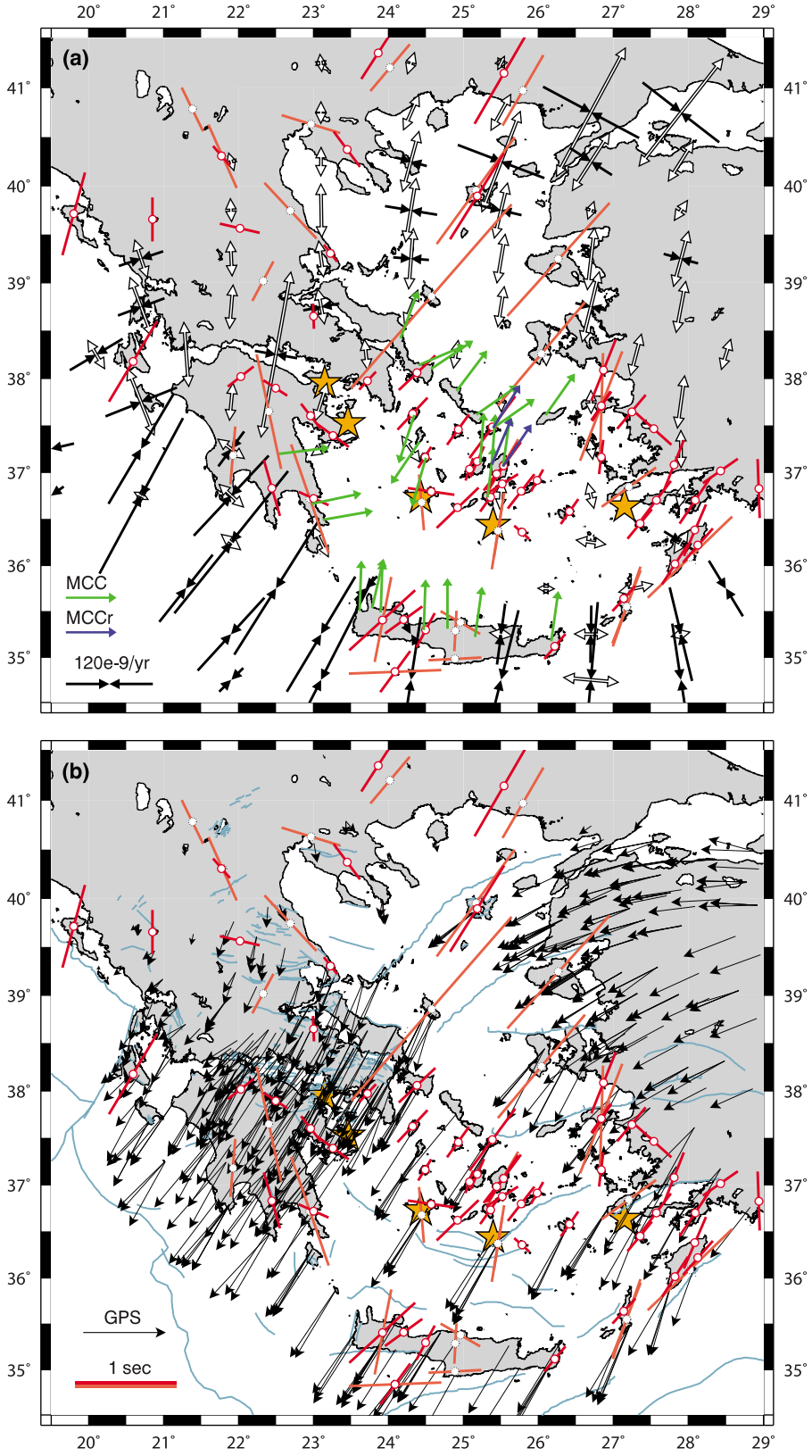
(a)
MCC
MCCr
120e-9/yr
(b)
GPS
1 sec
20°
21°
22°
23°
24°
25°
26°
27°
28°
29°
41°
40°
39°
38°
37°
36°
35°

Figure 7

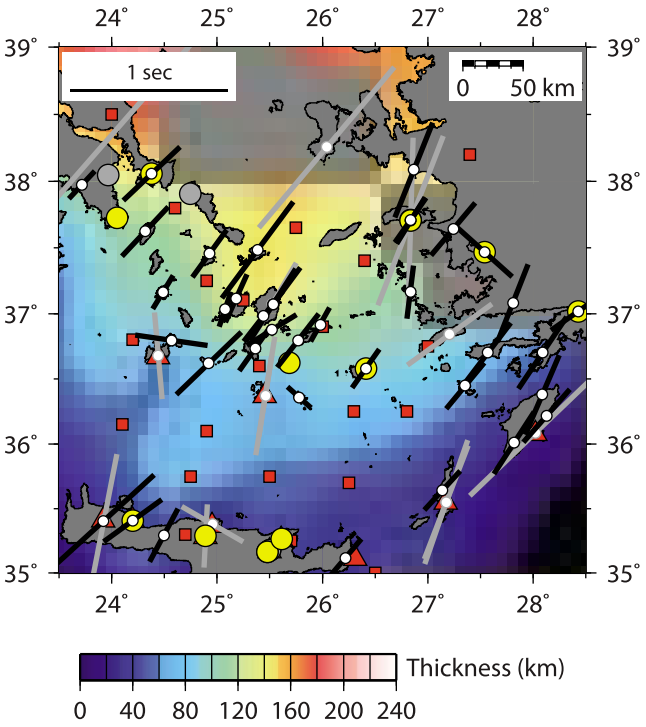

Figure 8. Map of average SKS splitting results (ϕ, δt) at each station (this study, black bars; previous study, gray bars) superimposed on a smoothed map of the separation between the Aegean Moho and the subducted African Moho calculated from the receiver function analysis of *Sodoudi et al.* [2006]. Orange triangles mark stations where the receiver function analysis estimated the African Moho depth, and orange squares mark centers of boxes where depths of African Moho were estimated from delay times of Sp conversions. Large yellow and gray circles indicate good null measurements by this and previous studies, respectively.

[22] For the westernmost termination of the trench, in the Ionian islands, we observe large delay times in Kefalonia Island, almost parallel to the transform fault (Figure 4). Anisotropy directions parallel to the strike of transform faults have been observed globally, and have been attributed to the vertical foliation and near-horizontal orientation of A axis parallel to the strike-slip motion [*Savage*, 1999, and references therein]. To the north of KTF, as the plate boundary is offset eastward and the collision of the Apulia platform and the northwestern Greece takes place, anisotropy measurements at Corfu Island show large delay times almost perpendicular to the convergence boundary (Figure 4). Comparable NNE-SSW directions in shear wave splitting have been found in the Apulian platform westward (Figure 4), and have been attributed to the fragmented subduction system in the mantle of this region [*Baccheschi et al.*, 2008]. Similarly, for the eastern side of the Apulian platform, various authors suggested the existence of a possible slab tear north of KTF [e.g., *Wortel and Spakman*, 2000; *Suckale et al.*, 2009]. The possibility of a toroidal mantle flow at the edge of the slab should also be investigated in the presence of future denser station measurements coverage.

[23] At the easternmost side of the Hellenic arc, between eastern Crete and southwestern Turkey, most of the measurements show anisotropy directions parallel to the trench (Figure 4). Estimates from a receiver function study in the area [*Sodoudi et al.*, 2006], although it is not very well sampled, reveal a mantle wedge with thickness between 40 km and 80 km (Figure 8). If the source of anisotropy is located above the descending slab, in the fore-arc mantle wedge, then it may be produced either from B-type LPO indicating a flow perpendicular to the trench similar to the back-arc area, or an A-type LPO indicating a flow parallel to the trench. *Long and Silver* [2008], based on anisotropy estimates globally, suggested that trenches dominated by slab retreat are more likely to have trench-parallel flow instead of B-type LPO. As the trench slab system migrates, the subslab mantle is forced around the slab edges and flows parallel to the trench. As material enters the mantle wedge, it increases in velocity because the flow is confined to a narrower region and it must replace the wedge material that is conductively cooled and removed by the slab subduction. Rapid flow into the wedge increases temperatures beneath the fore arc, which favors A-type LPO and thus trench-parallel anisotropy caused by flow rather than B-type LPO. *Brun and Sokoutis* [2010] implied that as the slab strike retreated from an ESE-WNW orientation 45 Ma to its current position, it must have been torn parallel to the plate convergence leading to mantle flow around the edge. This slab tear may be located, as tomography studies reveal, somewhere below southwestern Turkey (Figure 9). Therefore, for the southeastern Hellenic trench, the anisotropy measurements probably reflect flow parallel to the trench below the slab, that enters the mantle wedge flowing around the slab edge. On the other hand, even if the thickness of the mantle wedge is too small to produce the observed anisotropy, especially close to southeastern corner of the Dodecanese, the existence of the subslab trench-parallel flow moving out of the way of the retreating slab could explain the measurements (Figure 9, cross section DD′).

[24] For the western part of the arc, beneath Peloponnese, our coverage is sparser (Figure 3). Anisotropy measurements there, although scattered, show a trend parallel to the trench (Figure 5). Mantle wedge anisotropy in the area

Figure 7. (a) Map of average SKS splitting results displayed at each station (red thin bars) superimposed with strain rates and metamorphic core complexes stretching lineations (MCC). Strain rates are averages for 0.6° × 0.5° grid areas after *Kreemer et al.* [2003]. Metamorphic core complexes stretching vectors are in green (MCC) for the present strike and in blue (MCCr) for their position restored for paleomagnetic rotations [*Jolivet et al.*, 2009, and references therein]. Orange stars indicate the active volcanic arc. (b) Similarly, map of average SKS splitting results superimposed with GPS displacement vectors and main faults. GPS displacement vectors relative to a stable Eurasia are by *Nyst and Thatcher* [2004], *Reilinger et al.* [2006], *Hollenstein et al.* [2008], and *Floyd et al.* [2010]. Main faults in light blue are similar with Figure 1.

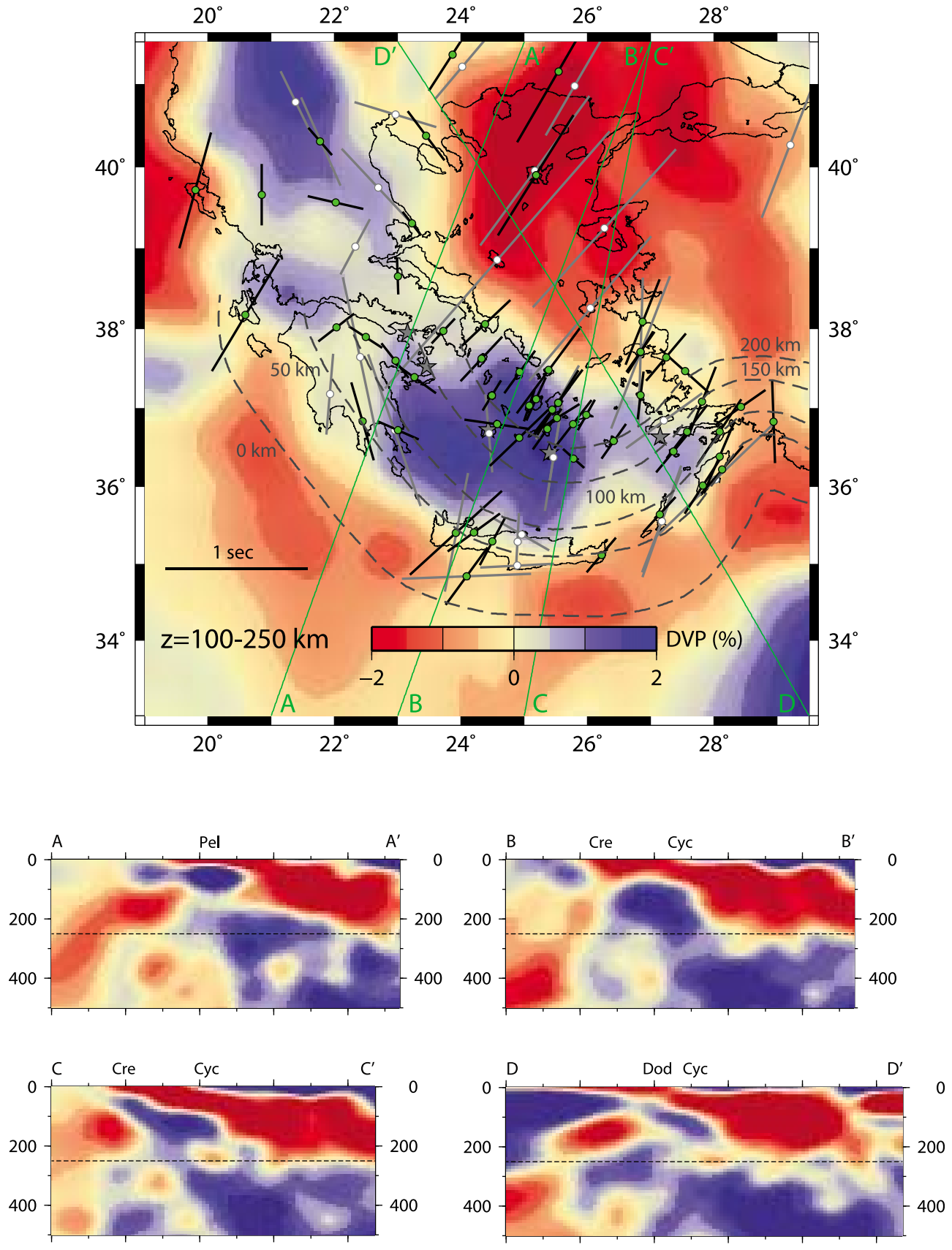
20°
22°
24°
26°
28°
40°
38°
36°
34°
D′
A′
B′
C′
50 km
0 km
100 km
150 km
200 km
1 sec
z=100-250 km
DVP (%)
−2
0
2
A
B
C
D
A
Pel
A′
B
Cre
Cyc
B′
C
Cre
Cyc
C′
D
Dod
Cyc
D′
0
200
400

Figure 9

would be less likely due to its small thickness (Figure 9, cross section AA′). Moreover, *Suckale et al.* [2009], on a teleseismic study from data of a SW-NE oriented temporary seismic array across the Hellenic arc, observed strong back azimuthal variations indicating that the lithospheric structure underneath the southern Peloponnese, deviates from the assumed 2-D geometry with isotropic material properties. Their observations from different seismic phases suggested that there is not strong seismic anisotropy in the mantle wedge. As previously suggested by *Jolivet et al.* [2009], we support the existence of a trench-parallel flow beneath the slab, that produces the observed anisotropy pattern. Deviations from the NNW-SSE trend parallel to the trench may be attributed to frozen-in lithospheric anisotropy due to the trench retreat since the Miocene [*Brun and Sokoutis*, 2010], which would require a more NW-SE strike orientation of trench-parallel flow.

[25] The observed anisotropy pattern changes from south Peloponesse toward Crete. Splitting observations in western Crete show similar NE-SW fast directions to the back-arc area (Figure 4). It is proposed that the western part of Crete is entering a continental collision stage [e.g., *Endrun et al.*, 2008], with no underlying mantle wedge. *Ganas and Parsons* [2009] supported this interpretation, with a deformation finite element model, showing that this area is the locus of the highest uplift rates within the arc. Moreover, *Rontogianni et al.* [2011], based on stress inversion of intermediate depth moment tensor solutions, suggested a stress regime of confined compression for the area. On the other hand, receiver functions analysis revealed a possible wedge thinner than 40 km in western Crete (Figure 8). In order to produce the observed delays the anisotropy layer should be thicker. Therefore, our preferred solution is that the observed anisotropy pattern has as a source the subslab mantle. If the slab was retreating, then the anisotropy directions should be parallel to the trench. However, as *Ganas and Parsons* [2009] suggested, the slab rollback is stalled at western Crete and, therefore, the entrained flow beneath the slab may be perpendicular to the trench and subparallel to the convergence direction (Figure 7), as simple models suggest [*Hall et al.*, 2000]. Although the origin of the observed anisotropy in western Crete is not so obvious, there is an evident change of the observed pattern from west to east (Figure 9, cross sections BB′ and CC′). Active source seismic tomography profiles along the island show a gradual developing mantle wedge toward the east [*Bohnhoff et al.*, 2001]. The area near central east Crete, where the transition occurs from a developing collisional regime to a subduction regime with mantle wedge [*Endrun et al.*, 2008], shows good nulls (Figure 3). Finally, at the easternmost tip of Crete the anisotropy direction becomes parallel to the trench in accordance with the observations further east in Dodecanese (Figure 4).

5. Conclusions

[26] Differences on the anisotropy parameters between this study and that of *Hatzfeld et al.* [2001] are mainly attributed on the different methods used for their computation, especially in the complex three-dimensional high curvature Hellenic trench. Additionally, the choice of acceptable results in this study is stricter due to a larger number of measurements and denser coverage in the south Aegean. There is not a uniform relationship between the observed anisotropy and the crustal velocity or strain field.

[27] The observed anisotropy in the back-arc area shows a gradual increase in delay times from south to north, with a prevailing NE-SW direction. This directional pattern is in agreement with GPS velocities and metamorphic core complexes restored for paleomagnetic rotations for the Cyclades area only. The origin of the anisotropy may be mantle wedge flow, induced by the retreating descending slab, but the coupling between mantle flow and the crustal motion deformation is not clear. A change of the prevailing anisotropy pattern is observed around the volcanic arc with fast directions subparallel to it and also good nulls. A tentative explanation is that this area marks the transition between the back-arc-induced anisotropy and the near-trench-induced anisotropy.

[28] For the Peloponnese area, although our coverage is sparser, we support the existence of a trench-parallel flow beneath the shallow-dipping slab. Some deviation from the NNW-SSE trend may reflect frozen-in lithospheric anisotropy as a result of trench retreat and clockwise rotation since the Miocene. At the westernmost termination of the trench, anisotropy fast directions are parallel to the Kefalonia Transform Fault. This may be attributed to foliation and LPO orientation parallel to the fault. However, the existence of similar measurements to the north, perpendicular to the convergence boundary, may be attributed to toroidal mantle flow around the fragmented slab edge in this region. For the western part of Crete, which enters a collisional stage, the source of anisotropy should lie beneath the slab. Contrary to other areas of the trench, the anisotropy is parallel to the direction of convergence. This is possibly due to a stall of the slab retreat there, that may cause an entrained flow beneath the slab, perpendicular to the trench. Good nulls at central east Crete indicate a change in the tectonic structure and the anisotropy origin, toward the east. The fast directions at the easternmost side of the Hellenic arc are trench parallel, reflecting a similar flow beneath the slab. If a suggested slab tear exists beneath southwestern Turkey, then

Figure 9. Average SKS splitting results (ϕ, δt) at each station (this study, black thin bars; previous study, gray thin bars) superimposed on the average Vp perturbation of the tomography model by *Piromallo and Morelli* [2002] for the topmost mantle between 100 km and 250 km depth. Gray dashed contours of the subducting slab after *Gudmundsson and Sambridge* [1998]. Green lines indicate the surface traces of cross sections through the model. The direction of plotting for the cross sections is from south to north, and each one is marked accordingly. Dashed horizontal lines in cross sections mark the upper 250 km where most of the anisotropy occurs in the mantle [*Savage*, 1999]. Regions discussed in the text are also marked at surface. Pel, Peloponnese; Cre, Crete; Cyc, Cyclades; Dod, Dodecanese.

a toroidal mantle flow around the edge of the slab may also produce trench-parallel flow within the mantle wedge.

[29] The results presented here used data recorded in a dense network in south Aegean for a time period of less than two years. The implementation of the Hellenic Unified Seismic Network (HUSN) with more than 120 stations as well as the analysis of local and regional S phases will offer additional data in the near future for a more complete picture of the crustal and upper mantle anisotropy of the region. The possibility of a toroidal mantle flow at both edges of the slab should also be investigated in the presence of future denser station measurements coverage.

[30] **Acknowledgments.** We are grateful to all the scientists and scientific personnel of the EGELADOS Working Group from Ruhr University Bochum, GeoForschungsZentrum Potsdam, Technical University of Istanbul, Technical University of Chania, Aristotle University of Thessaloniki, and National Observatory of Athens who participated in the field programs of 2005–2007. This study was supported by the National Science Council of Taiwan, under grant NSC99-2119-M-001-024 and the Network of European Research Infrastructures for Earthquake Risk Assessment and Mitigation (NERA), an EU project financed under FP-7 grant 262330 (CP-CSA_INFRA-2010-1.1.27). SKS measurements from previous studies were easily accessed from the Splitting Database [*Wüstefeld et al.*, 2009]. The GMT mapping software [*Wessel and Smith*, 1998] was used for the preparation of the figures in this paper. Part of the analysis is done using the Seismic Analysis Code (SAC) developed by the Lawrence Livermore National Laboratory. We are indebted to the Associate Editor and two anonymous reviewers for their constructive comments that improved the initial version of this manuscript.

References

Baccheschi, P., L. Margheriti, and M. Steckler (2007), Seismic anisotropy reveals focused mantle flow around Calabrian slab (southern Italy), *Geophys. Res. Lett.*, *34*, L05302, doi:10.1029/2006GL028899.

Baccheschi, P., L. Margheriti, and M. Steckler (2008), SKS splitting in southern Italy: Anisotropy variations in a fragmented subduction zone, *Tectonophysics*, *462*, 49–67, doi:10.1016/j.tecto.2007.10.014.

Behn, M. D., G. Hirth, and P. B. Kelemen (2007), Trench-parallel anisotropy produced by foundering of arc lower crust, *Science*, *317*, 108–111.

Bohnhoff, M., J. Makris, D. Papanikolaou, and G. Stavrakakis (2001), Crustal investigation of the Hellenic subduction zone using wide aperture seismic data, *Tectonophysics*, *343*, 239–262.

Brun, J.-P., and G. Sokoutis (2010), 45 M.y of Aegean crust and mantle flow from driven by trench retreat, *Geology*, *38*(9), 815–818.

Buontempo, L., G. H. R. Bokelmann, G. Barruol, and J. Morales (2008), Seismic anisotropy beneath southern Iberia from SKS splitting, *Earth Planet. Sci. Lett.*, *273*, 237–250.

Chamot-Rooke, N., et al. (2005), DOTMED-Deep Offshore Tectonics of the Mediterranean: A synthesis of deep marine data in eastern Mediterranean, *Mem. Soc. Geol. Fr.*, *177*, 1–64.

Currie, C. A., J. F. Cassidy, R. D. Hyndman, and M. G. Bostock (2004), Shear wave anisotropy beneath the Cascadia subduction zone and western North American craton, *Geophys. J. Int.*, *157*, 341–353, doi:10.1111/j.1365-246X.2004.02175.x.

Endrun, B., T. Meier, S. Lebedev, M. Bohnhoff, G. Stavrakakis, and H.-P. Harjes (2008), S velocity structure and radial anisotropy in the Aegean region from surface wave dispersion, *Geophys. J. Int.*, *174*, 593–616, doi:10.1111/j.1365-246X.2008.03802.x.

Faccenna, C., O. Bellier, J. Martinod, C. Piromallo, and V. Regard (2006), Slab detachment beneath eastern Anatolia: A possible cause for the formation of the North Anatolian Fault, *Earth Planet. Sci. Lett.*, *242*, 85–97.

Floyd, M. A., et al. (2010), A new velocity field for Greece: Implications for the kinematics and dynamics of the Aegean, *J. Geophys. Res.*, *115*, B10403, doi:10.1029/2009JB007040.

Friederich, W., and T. Meier (2008), Temporary seismic broadband network acquired data on Hellenic subduction zone, *Eos Trans. AGU*, *89*(40), doi:10.1029/2008EO400002.

Fukao, Y. (1984), Evidence from core-reflected shear wave anisotropy in the Earth's mantle, *Nature*, *309*, 695–698.

Ganas, A., and T. Parsons (2009), Three-dimensional model of Hellenic arc deformation and origin of the Cretan uplift, *J. Geophys. Res.*, *114*, B06404, doi:10.1029/2008JB005599.

Gudmundsson, O., and M. Sambridge (1998), A regionalized upper mantle (RUM) seismic model, *J. Geophys. Res.*, *103*, 7121–7136.

Hall, C., K. Fischer, A. R. Parmentier, and D. K. Blackman (2000), The influence of the plate motions on three-dimensional back arc mantle flow and shear wave splitting, *J. Geophys. Res.*, *105*, 28,009–28,033.

Hatzfeld, D., et al. (2001), Shear wave anisotropy in the upper mantle beneath the Aegean related to internal deformation, *J. Geophys. Res.*, *106*, 30,737–30,753.

Hollenstein, C., M. Mueller, A. Geiger, and H.-G. Kahle (2008), Crustal motion and deformation in Greece from a decade of GPS measurements, 1993-2003, *Tectonophysics*, *449*, 17–40, doi:10.1016/j.tecto.2007.12.006.

Huguen, C., J. Mascle, E. Chaumillon, J. M. Woodside, J. Benkhelil, A. Kopf, and A. Volkonskaa (2001), Deformational styles of the eastern Mediterranean Ridge and surroundings from combined swath mapping and seismic reflection profiling, *Tectonophysics*, *343*, 21–47, doi:10.1016/S0040-1951(01)00185-8.

Jolivet, L., C. Faccenna, and C. Piromallo (2009), From mantle to crust: Stretching the Mediterranean, *Earth Planet. Sci. Lett.*, *285*, 198–209, doi:10.1016/j.epsl.2009.06.017.

Jung, H., and S.-I. Karato (2001), Water-induced fabric transitions in olivine, *Science*, *293*, 1460–1463.

Karato, S., and P. Wu (1993), Rheology of the upper mantle: A synthesis, *Science*, *260*, 771–778.

Konstantinou, K. I., and N. S. Melis (2008), High-frequency shear-wave propagation across the Hellenic subduction zone, *Bull. Seismol. Soc. Am.*, *98*, 797–803.

Kreemer, C., and N. Chamot-Rooke (2004), Contemporary kinematics of the southern Aegean and the Mediterranean Ridge, *Geophys. J. Int.*, *157*, 1377–1392, doi:10.1111/j.1365-246X.2004.02270.x.

Kreemer, C., W. Holt, and A. Haines (2003), An integrated global model of present-day plate motions and plate boundary deformation, *Geophys. J. Int.*, *154*, 8–34.

Kreemer, C., N. Chamot-Rooke, and X. Le Pichon (2004), Constraints on the evolution and vertical coherency of deformation in the northern Aegean from a comparison of geodetic, geologic and seismologic data, *Earth Planet. Sci. Lett.*, *225*, 329–346, doi:10.1016/j.epsl.2004.06.018.

Le Pichon, X., and C. Kreemer (2010), The Miocene-to-present kinematic evolution of the eastern Mediterranean and Middle East and its implications for dynamics, *Annu. Rev. Earth Planet. Sci.*, *38*, 323–351.

Levin, V., D. Okaya, and J. Park (2007), Shear wave birefringence in wedge-shaped anisotropic regions, *Geophys. J. Int.*, *168*, 275–286, doi:10.1111/j.1365-246X.2006.03224.x.

Long, M. D., and T. W. Becker (2010), Mantle dynamics and seismic anisotropy, *Earth Planet. Sci. Lett.*, *297*, 341–354.

Long, M. D., and P. G. Silver (2008), The subduction zone flow field from seismic anisotropy: A global view, *Science*, *319*, 315–319.

Louvari, E., A. A. Kiratzi, and B. C. Papazachos (1999), The Cephalonia Transform Fault and its extension to western Lefkada Island (Greece), *Tectonophysics*, *308*, 223–236.

Maupin, V., and J. Park (2007), Theory and observations: Wave propagation in anisotropic media, in *Treatise on Geophysics*, edited by G. Schubert, pp. 289–321, Elsevier, New York, doi:10.1016/B978-044452748-6.00007-9.

McClusky, S., et al. (2000), Global Positioning System constraints on plate kinematics and dynamics in the eastern Mediterranean and Caucasus, *J. Geophys. Res.*, *105*, 5695–5719.

Meijer, P. T., and M. G. R. Wortel (1996), Temporal variation in the stress field of the Aegean region, *Geophys. Res. Lett.*, *23*, 439–442.

Monteiller, V., and S. Chevrot (2010), How to make robust splitting measurements for single-station analysis and three-dimensional imaging of seismic anisotropy, *Geophys. J. Int.*, *182*, 311–328, doi:10.1111/j.1365-246X.2010.04608.x.

Morris, A., and M. Anderson (1996), First palaeomagnetic results from the Cycladic Massif, Greece, and their implications for Miocene extension directions and tectonic models in the Aegean, *Earth Planet. Sci. Lett.*, *142*, 397–408.

Nakajima, J., and A. Hasegawa (2004), Shear-wave polarization anisotropy and subduction-induced flow in the mantle wedge of northeastern Japan, *Earth Planet. Sci. Lett.*, *225*, 365–377, doi:10.1016/j.epsl.2004.06.011.

Nyst, M., and W. Thatcher (2004), New constraints on the active tectonic deformation of the Aegean, *J. Geophys. Res.*, *109*, B11406, doi:10.1029/2003JB002830.

Papazachos, B., V. Karakostas, C. Papazachos, and E. Skordilis (2000), The geometry of the Wadati-Benioff zone and lithospheric kinematics in the Hellenic arc, *Tectonophysics*, *319*, 275–300.

Piromallo, C., and A. Morelli (2002), *P* wave tomography of the mantle under the Alpine-Mediterranean area, *J. Geophys. Res.*, *108*(B2), 2065, doi:10.1029/2002JB001757.

Rau, R.-J., W.-T. Liang, H. Kao, and B.-S. Huang (2000), Shear wave anisotropy beneath the Taiwan orogen, *Earth Planet. Sci. Lett.*, *177*, 177–192, doi:10.1016/S0012-821X(00)00058-3.

Reilinger, R., et al. (2006), GPS constraints on continental deformation in the Africa-Arabia-Eurasia continental collision, *J. Geophys. Res.*, *111*, B05411, doi:10.1029/2005JB004051.

Rontogianni, S., K. I. Konstantinou, N. S. Melis, and C. P. Evangelidis (2011), Slab stress field in the Hellenic subduction zone as inferred from intermediate depth earthquakes, *Earth Planets Space*, *63*(2), 139–144, doi:10.5047/eps.2010.11.011.

Savage, M. S. (1999), Seismic anisotropy and mantle deformation: What have we learned from shear wave splitting?, *Rev. Geophys.*, *37*(1), 65–106.

Schmid, C., S. Van der Lee, and D. Giardini (2004), Delay times and shear wave splitting in the Mediterranean region, *Geophys. J. Int.*, *159*, 275–290, doi:10.1111/j.1365-246X.2004.02381.x.

Smith, P. G., D. A. Wiens, K. M. Fischer, L. M. Dorman, S. C. Webb, and J. A. Hilderbrand (2001), A complex pattern of mantle flow in the Lau back arc, *Science*, *292*, 713–716.

Sodoudi, F., et al. (2006), Lithospheric structure of the Aegean obtained from P and S receiver functions, *J. Geophys. Res.*, *111*, B12307, doi:10.1029/2005JB003932.

Spakman, W., M. G. R. Wortel, and N. J. Vlaar (1988), The Hellenic subduction zone: A tomographic image and its geodynamic implications, *Geophys. Res. Lett.*, *15*, 60–63.

Suckale, J., S. Rondenay, M. Sachpazi, M. Charalampakis, A. Hosa, and L. H. Royden (2009), High-resolution seismic imaging of the western Hellenic subduction zone using teleseismic scattered waves, *Geophys. J. Int.*, *178*, 775–791, doi:10.1111/j.1365-246X.2009.04170.x.

Taymaz, T., J. Jackson, and D. McKenzie (1991), Active tectonics of the north and central Aegean Sea, *Geophys. J. Int.*, *106*, 433–490.

Vinnik, L. P., V. Farra, and B. Romanowicz (1989), Azimuthal anisotropy in the Earth from observations of SKS at Geoscope and Nars broadband stations, *Bull. Seismol. Soc. Am.*, *79*, 1542–1558.

Wessel, P., and W. H. F. Smith (1998), New, improved version of the Generic Mapping Tools released, *Eos Trans. AGU*, *79*(47), 579.

Wolfe, C., and S. Solomon (1998), Shear-wave splitting and implications for mantle flow beneath the MELT region of the East Pacific Rise, *Science*, *280*, 1230–1232.

Wortel, M. J. R., and W. Spakman (2000), Subduction and slab detachment in the Mediterranean-Carpathian region, *Science*, *290*, 1910–1917.

Wüstefeld, A., G. H. R. Bokelmann, G. Barruol, and J.-P. Montagner (2009), Identifying global seismic anisotropy patterns by correlating shear-wave splitting and surface waves data, *Phys. Earth Planet. Inter.*, *176*(3–4), 198–212, doi:10.1016/j.pepi.2009.05.006.

C. P. Evangelidis and N. S. Melis, Institute of Geodynamics, National Observatory of Athens, Lofos Nimfon, Athens 11810, Greece. (cevan@noa.gr)

K. I. Konstantinou, Institute of Geophysics, National Central University, Jhongli 32001, Taiwan.

W.-T. Liang, Institute of Earth Sciences, Academia Sinica, Taipei 11529, Taiwan.